Correlation between suprathermal electron bursts, broadband extremely low frequency waves, and local ion heating in the midaltitude cleft//low-latitude boundary layer observed by Cluster

Y.V. Bogdanova, A.N. Fazakerley, C.J. Owen, B. Klecker, N. Cornilleau-Wehrlin, B. Grison, M. André, P. Cargill, H. Rème, J.M. Bosqued, et al.

Correlation between suprathermal electron bursts, broadband extremely low frequency waves, and local ion heating in the midaltitude cleft/low-latitude boundary layer observed by Cluster

Y. V. Bogdanova,[1] A. N. Fazakerley,[1] C. J. Owen,[1] B. Klecker,[2] N. Cornilleau-Wehrlin,[3] B. Grison,[3] M. André,[4] P. Cargill,[5] H. Rème,[6] J. M. Bosqued,[6] L. M. Kistler,[7] and A. Balogh[5]

Received 23 April 2004; revised 23 September 2004; accepted 28 October 2004; published 30 December 2004.

[1] The Cluster spacecraft often cross the midaltitude cleft/cusp and observe a very well defined ''electron-only cleft'' region consisting of electron injections without magnetosheath ions. This region contains soft suprathermal (<500 eV) electron bursts in antifield and/or field-aligned directions. We present an example of such observations which shows that the O^+ ion outflow at midaltitudes appears just poleward of the open-closed boundary simultaneously with electron injections and was observed in the cleft, cusp, and mantle in the form of narrow energy beam. Inside the ''electron-only'' cleft the suprathermal electron bursts are strongly correlated with strong O^+ and H^+ ion heating and with localized extra low frequency (ELF) (1–10 Hz) magnetic field wave power with broadband spectra. Our study shows that strong ion heating was observed only in the region with electron field-aligned anisotropy more than 2. In addition, comparison of particle data from two spacecraft, which crossed the heating region with a time difference of 4 min, shows the correlation between ion outflow fluxes and fluxes of the injected electrons. Whereas ELF electromagnetic waves are localized inside the ion heating region, ELF electrostatic waves are detected throughout the cleft/cusp/mantle regions, where strong ion heating was not observed, suggesting that electromagnetic ELF waves heat ions in the cleft region. Owing to the absence of magnetosheath ions and strong field-aligned currents, we suppose that inside ''electron-only'' cleft region the suprathermal electron bursts are most likely an energy source for the wave destabilization. We suggest that the location of the heating region and the level of the outflow ion fluxes could be related to electron injection in the cleft in such events. *INDEX TERMS:* 2724 Magnetospheric Physics: Magnetopause, cusp, and boundary layers; 2736 Magnetospheric Physics: Magnetosphere/ionosphere interactions; 7807 Space Plasma Physics: Charged particle motion and acceleration; 7867 Space Plasma Physics: Wave/particle interactions; *KEYWORDS:* cleft electron observations, dayside ion outflow, ion heating in the cleft/cusp, wave/particle interaction

Citation: Bogdanova, Y., et al. (2004), Correlation between suprathermal electron bursts, broadband extremely low frequency waves, and local ion heating in the midaltitude cleft/low-latitude boundary layer observed by Cluster, *J. Geophys. Res.*, *109*, A12226, doi:10.1029/2004JA010554.

1. Introduction

[2] Since it was first reported by *Lockwood et al.* [1985], ionospheric oxygen outflow from the cleft/cusp region has been extensively studied using data from various satellites. Ion outflow from the dayside ionosphere also has been studied at low altitudes using radar data [e.g., *Nilsson et al.*, 1998; *Ogawa et al.*, 2003; *McCrea et al.*, 1991; *McCrea et al.*, 2000] and it was suggested that three main possible mechanisms could drive ion outflow: frictional (Joule) ion heating, thermal electron heating, and ambipolar electric field. It has been shown that dayside outflow is one of the main sources of magnetospheric heavy ion populations (see reviews by *Moore et al.* [1999a] and *André and Yau* [1997]). On the basis of simultaneous observations of the outflow by EISCAT Svalbard radar and DMSP satellites, *Ogawa et al.* [2003] found that outflow was observed in the cleft, cusp, and mantle. *Lockwood et al.* [1985] showed that this outflow is a persistent phenomenon. *Valek et al.* [2002] presented statistical study of the ionospheric outflow and cusp position based on Polar data and show that outflow begins in the cleft ~1.5° equatorward of the cusp boundary

[1]Mullard Space Science Laboratory, University College London, Surrey, UK.
[2]Max-Planck Institute fur Extraterrestrische Physik, Garching, Germany.
[3]Centre d'Etude des Environnements Terrestre et Planetaires, Velizy, France.
[4]Swedish Institute of Space Physics, Uppsala, Sweden.
[5]Space and Atmospheric Physics, Imperial College, London, UK.
[6]Centre d'Etude Spatiale des Rayonnements, Toulouse, France.
[7]Space Science Center, University of New Hampshire, Durham, New Hampshire, USA.

0148-0227/04/2004JA010554

at a point that coincides with the open-closed field line boundary and it peaks at the cusp boundary and extends another 4–5° poleward in the cusp. It was suggested [*Lockwood et al.*, 1985] that upflowing ions are accelerated in a rather narrow latitudinal region in the cleft and are then swept in the antisunward direction under the effect of the convection electric field. The ions become spatially dispersed across the polar cap according to time of flight and form a "cleft ion fountain." Many studies have confirmed that this ion outflow source is located inside the cleft region and have estimated the latitudinal size of the heating region as 1.5°–2° [e.g., *Dubouloz et al.*, 1998; *Bogdanova et al.*, 2004]. SCIFER rocket measurements at 1400 km reveal that this region, named the heating wall, contains transversely accelerated ions (TAI) and can be very narrow (30–40 km width at 1400 km altitude) [*Arnoldy et al.*, 1996]. However, *Dubouloz et al.* [2001] presented one event study showing that the heating region likely coincides with the polar cusps. The source is rather broad in longitude, a few hours in MLT [e.g., *Bouhram et al.*, 2002]. Upwelling ions with conic distributions have been observed at altitudes from 1400 km [*Arnoldy et al.*, 1996] to >4 R_E (e.g., this paper). Previous works showed that the heating region could extend from the ionosphere level till 3 R_E, and there is height-integrated energization of the ions [e.g., *Dubouloz et al.*, 2001; *Bouhram et al.*, 2002; *Bouhram et al.*, 2003].

[3] Inside the source region, many observations (see review by *Moore et al.* [1999a]) have shown strong localized perpendicular energization of the ions. *André et al.* [1990, 1998] and *Norqvist et al.* [1998] have shown that perpendicular acceleration of the ions in this region and outflow are correlated mainly with broadband extremely low frequency (BBELF) wave power in the frequency band from below 1 Hz up to 1 kHz, which includes Alfvén waves, ion acoustic waves, electrostatic solitary waves, and electrostatic ion cyclotron waves. Correlations between heated ions and electromagnetic ion cyclotron (EMIC) waves and/or lower hybrid waves have also been presented [*Moore et al.*, 1999a]. It was suggested that all these wave modes could potentially heat ions via resonant interaction near ions gyrofrequencies. Ions will be heated by left-hand polarized fraction of the electric field wave. However, the definitive identification of the wave modes responsible for ion heating is still an open issue.

[4] The one major question is a free source of energy for wave growth. Numerous observations show that in the cusp/cleft region, as well as in the nightside auroral region, ion heating and enhancement of low-frequency wave power coincide with field-aligned electron precipitation. *Johnstone and Winningham* [1982] first presented this observation for the auroral region and showed that these soft (<500 eV) electron injections are broadband in energy, often highly field-aligned, and occur on very small spatial scales (2–6 s). Close correlation between suprathermal electron bursts, BBELF turbulence, and ion heating and outflow were observed inside the cleft/cusp at lower (1400–1700 km) altitudes by SCIFER rocket [*Pollock et al.*, 1996; *Arnoldy et al.*, 1996] and Freja satellite [*Knudsen et al.*, 1998; *Norqvist et al.*, 1998] and it was suggested that the suprathermal electron bursts could be the free energy source for the waves. In the ionosphere level, *Ogawa et al.* [2003] showed that ion upflow events are associated with relatively high soft electron precipitation. Theoretical studies [*Temerin and Lysak*, 1984; *Gustafsson et al.*, 1990] also proved that electron beams could generate most of the wave modes observed in the cleft/cusp. However, correlation between magnetosheath downflowing ion beams and the ion heating and outflow also have been observed [*Norqvist et al.*, 1998; *Nilsson et al.*, 1998; *Bouhram et al.*, 2002]. Field-aligned currents in the cleft/cusp have also been suggested as a potential wave energy source [*Yau et al.*, 1983; *Strangeway et al.*, 2000].

[5] It was shown that the location of the ion outflow source region and outflow fluxes are correlated with interplanetary magnetic field IMF B_y and B_z components, solar wind velocity and density [*Pollock et al.*, 1990; *Oeroset et al.*, 2000; *Miyake et al.*, 2002], with solar wind pressure pulses [*Moore et al.*, 1999b; *Fuselier et al.*, 2002], and with geomagnetic activity [*Oeroset et al.*, 2000]. *Strangeway et al.* [2000], on the basis of FAST observations, suggested that reconnection near the magnetospheric cusp controls the ion outflow via downward electromagnetic Poynting flux.

[6] During crossings of the midaltitude cleft/cusp region, the Cluster spacecraft frequently observe a region poleward of the open-closed boundary (OCB) containing unidirectional or bidirectional beams of soft magnetosheath-like electrons without magnetosheath protons injections. This region begins at the OCB and extends over <0.2° ILAT near noon and up to 2° ILAT in the dawn and dusk sectors. Inside the electron-only cleft near the OCB, a region of localized ion transverse heating is usually observed. The investigation of such events, with well-separated electron and ion edges of the cleft/cusp, could be very promising, as we can examine the relative roles of the magnetosheath electrons and ions in the wave generation and ion local heating processes inside the cleft/cusp. We have studied five events with similar properties and discuss here the clearest event using data from two Cluster spacecraft. We should clarify that we do not address processes at the ionosphere level and the actual source for ion outflow but present Cluster observations inside the midaltitude cusp and discuss local ion heating at midaltitudes.

[7] The particle data come from the High Energy Electron Analyzer (HEEA) of the Plasma Electron and Current Experiment (PEACE) [*Johnstone et al.*, 1997] and Composition and Distribution Function (CODIF) sensor of the Cluster Ion Spectrometry experiment (CIS) [*Rème et al.*, 2001]. We also use magnetic field data from the Flux Gate Magnetometer (FGM) [*Balogh et al.*, 2001], wave data from the Electric Field and Wave (EFW) experiment [*Gustafsson et al.*, 2001], and the Spatio-Temporal Analysis of Field Fluctuations (STAFF) experiment [*Cornilleau-Wehrlin et al.*, 2003].

2. Observations

[8] At 1240 UT on 23 August 2001, Cluster spacecraft 4 (C4) was located at [3.3, −0.8, 3.5] R_E in the GSE coordinate system, at an altitude of 3.9 R_E, outbound after a perigee pass. Cluster 1 (C1) was following a parallel track, displaced sunward by about a third of an R_E. During a 30-min interval 1245–1315 UT, C4 and C1 crossed the northern midaltitude polar region and observed three distinct regions: the cleft/low-latitude boundary layer

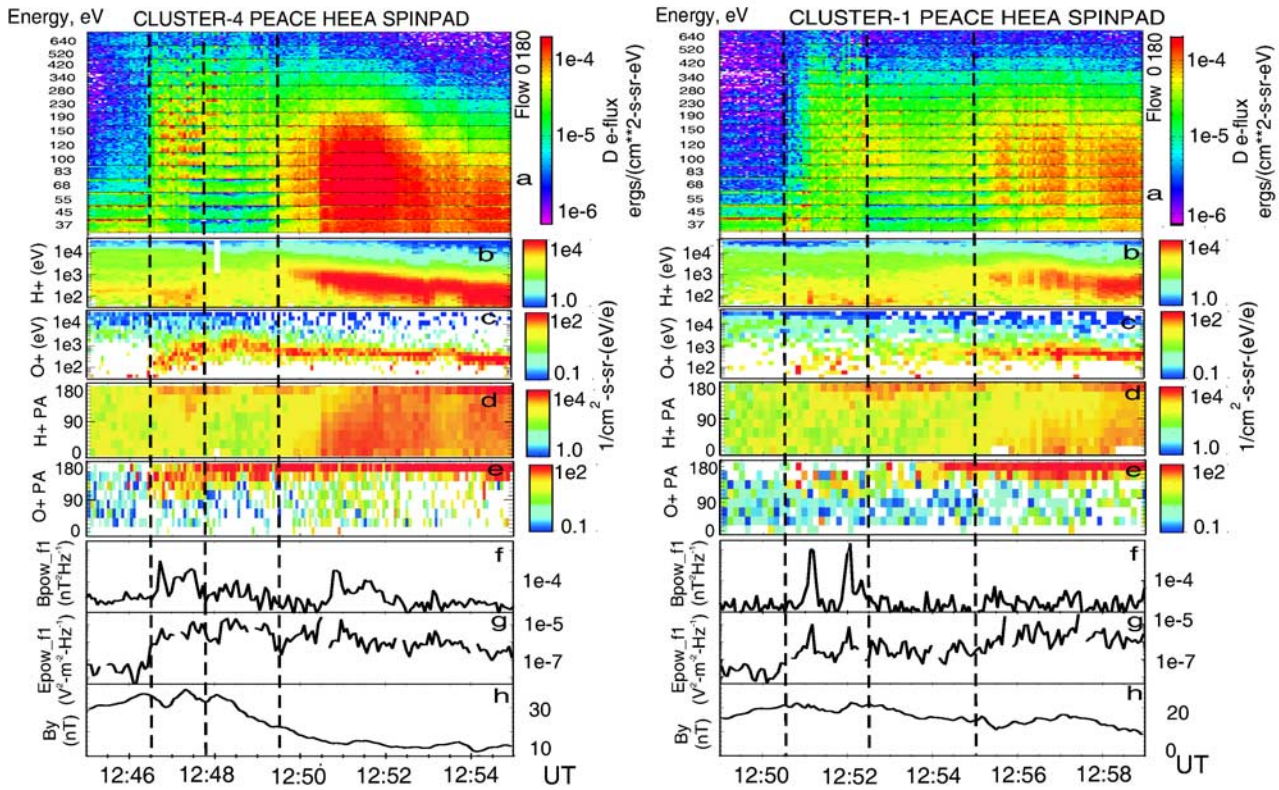

Figure 1. Plasma Electron and Current Experiment (PEACE)- High Energy Electron Analyzer (HEEA), Cluster Ion Spectrometry (CIS)-Composition and Distribution Function (CODIF), Flux Gate Magnetometer (FGM), Electric Field and Wave (EFW), and Spatio-Temporal Analysis of Field Fluctuations (STAFF) data on 23 August 2001, 1245–1255 UT, spacecraft 4 (left column), and 1249–1259 UT, spacecraft 1 (right column). Top panel in each column shows PEACE HEEA data for 15 energy bins in the range 32–700 eV. Each row in the plot presents the pitch angle distribution (0°–180°) for electrons with center energy shown on the left. Differential energy flux is color-coded according to the logarithmic color bar shown on the right, using the same scales for both spacecraft. Four middle panels display data from the CIS-CODIF instrument: H^+ energy-time spectrogram (b); O^+ energy-time spectrogram (c); H^+ and O^+ pitch angle (0°–180°) spectrograms (d, e). Differential energy flux again is color-coded using the same scale for both spacecraft. Panel f shows the magnetic field power spectral density for combined parallel and perpendicular components (with respect to spin axis) in the frequency band 1–10 Hz measured by the STAFF instrument. Panel g displays the EFW electric field power spectral density in the spin plane in the same frequency band, 1–10 Hz. Last panel shows the GSE B_Y component of the magnetic field obtained from FGM. The first dashed lines mark the open-closed boundary or equatorward edge of the electron low-latitude boundary layer. The second dashed line indicates the northward boundary of the local perpendicular heating region, and the third dashed line marks the equatorward boundary of the ion cleft. The equatorward boundary of the cusp proper lies at 1250:30 for spacecraft 4 and 1259:00 for spacecraft 1, as is apparent from the intensification of electron and ion fluxes after that time.

(hereafter referred to as cleft/LLBL), the cusp proper, and the mantle [*Newell and Meng*, 1998]. The time delay between observation of the OCB by C4 and C1 was ~4 min. The IMF (measured by ACE and shifted by the solar wind convection time, ~60 min) during the time of interest was steady and directed southward, with average values of $B_X \sim -2$ nT, $B_Y \sim -2$ nT, $B_Z \sim -1$ nT, such that we expect subsolar reconnection and antisunward convection in the polar cap. However, geomagnetic activity was quite low, $K_p = 1$ for the 3 hour period 0900 to 1200 and $K_p = 2$- for the period 1200 to 1500.

[9] An overview of the particle data (spin resolution, 4 s) from the PEACE and CIS instruments and field/wave data from the FGM, EFW and STAFF instruments is shown in Figure 1. The left panels correspond to C4 observations from 1245 to 1255 UT, and the right panels correspond to C1 data from 1249 to 1259 UT. Panel a in each column presents PEACE HEEA data in the measured energy range 30–700 eV. The spacecraft potential varied in the range 20–30 eV during this interval. Each subpanel shows a pitch angle distribution (0°–180°) for the energy channel centered on the value given on the left of the panel. In this case, pitch angle 0°/180° corresponds to downgoing/upgoing electrons. The differential energy flux of electrons is coded according to the logarithmic color bar on the right, with common scales for both spacecraft. The next four

panels in each column display data from CIS/CODIF, showing the H^+ energy-time spectrogram (panel b), the O^+ energy-time spectrogram (c), the H^+ pitch-angle spectrogram (d), and the O^+ pitch-angle spectrogram (e). Again, 0°/180° pitch angle corresponds to downgoing/upgoing ions and differential energy flux is color-coded with the same scales for both spacecraft. Panel f shows the magnetic field power spectral density for combined parallel and perpendicular (with respect to spin axis) components in the frequency band 1–10 Hz, measured by the STAFF instrument. Panel g displays the EFW spin plane electric field power spectral density in the same frequency band. We present here only these low-frequency bands which contain the proton gyrofrequency during this interval: $f_{H+} \sim 6.0$ Hz. The oxygen gyrofrequency is $f_{O+} \sim 0.4$ Hz and the electron gyrofrequency is ~12 kHz. The final panel shows the GSE B_y component of the FGM magnetic field. The magnetic field was directed mainly in the Z and X directions (GSE), so variations in the B_y component can be used as an indicator of field-aligned currents/Alfvén waves.

[10] At the beginning of the interval shown, C4 (left panels) is on closed field lines, and observes a high-energy electron population typical of trapped electrons of central plasma sheet origin (above the energy range shown here). At 1246:30 UT, MLT = 1352, ILAT = 78.2°, (first vertical dashed line) these trapped particles disappear and shortly afterward C4 observes structured injections of soft magnetosheath-like electrons (<500 eV) indicating that C4 crosses the OCB and enters the cleft/LLBL. From 1246:30 to 1250:30 UT, C4 crosses the cleft/LLBL, after which it enters the cusp proper, where much higher fluxes of protons and electrons are seen over a broad range of pitch angles. The cleft/LLBL is not occupied by precipitating magnetosheath ions until as late as 1249:30 UT. Throughout most of the electron-only interval, there is a fairly steady flux of electrons at all pitch angles except near the loss cone (180°) at levels of about 2×10^{-5} ergs $(cm^2\ s\ sr\ eV)^{-1}$. In addition, for much of the first 75 s that C4 is in the cleft/LLBL (1246:30–1247:45 UT, on Figure 1 time interval between first and second dashed lines), downgoing electrons are seen at fluxes a factor 5 to 10 higher, much of the time distributed across pitch angles 0° to 90°, mainly in the form of short-duration beams. There are also a few short-lived upgoing beams at similarly high fluxes, with pitch angles within 45° of the magnetic field. The integrated field-aligned electron number flux is relatively high, a few times 10^7 $(cm^2\ s\ sr)^{-1}$. During this interval (1246:30–1247:45 UT), ionospheric H^+ and O^+ ion outflow is observed (panels d and e). H^+ ions generally appear with pitch angles 150°–180°, consistent with upward motion from a transverse heating event below Cluster. Strong local proton transverse heating at Cluster altitudes is indicated by fluxes at all pitch angles from 90° to 180° in the interval 1247:15–1247:30 UT. For the first 75 s inside the cleft, O^+ ions appear with pitch angles 90°–180°. Study of the oxygen velocity distribution functions (not shown) shows the strong transverse oxygen energization, indicating that Cluster crossed the heating region during this time. The energy of the upwelling O^+ ions sharply increases from a few tens of eV to a value of 1 keV within this equatorward part of the cleft/LLBL. After 1247:45 UT (second dashed line) there is no evidence of local ion heating and the outflowing O^+ ion distributions evolve toward a field-aligned beam over the next 105 s inside the electron-only cleft/LLBL. A gradual decline of energy is also seen, interrupted by an interval lasting about a minute where energies reach as high as 2 keV, presumably a response to transiently enhanced heating below Cluster. During this crossing of the remaining electron-only cleft/LLBL, the occurrence rate and intensity of the beam-like electron fluxes decreases while the more isotropic lower flux background persists. Note that the strong local ion transverse energization (with 90° pitch-angle ions) occurs only inside the equatorward part of the electron-only cleft/LLBL, the region with relatively high fluxes of mainly downward electron beams.

[11] Just after crossing the OCB, the electric field instrument detects a sharp and long-lasting increase of the electric fluctuation in the frequency range 1–10 Hz, by a factor ~100. In addition, several brief periods with wave power a factor of 10 higher are seen in the cleft. Magnetic field fluctuations in the same frequency range appear shortly after the OCB crossing and show several periods of enhanced power during the cleft crossing. The strongest peaks are centered at 1246:45 UT and 1247:20 UT, concurrent with the two intervals of local transverse ion energization and strong fluxes of downward traveling electrons. These observations are consistent with the scenario of an electromagnetic wave playing a role in local transverse ion heating. The high-resolution STAFF data (not presented) show broadband spectra of the low-frequency electromagnetic waves. The B_y component of the magnetic field shows small-scale (5 nT) periodic variations inside the ion heating region, indicating the presence of weak filamentary field-aligned currents or Alfvén waves.

[12] At 1249:30 UT, MLT = 1357, ILAT = 78.9° (indicated by the third dashed line), C4 begins to see downgoing field-aligned protons, and 1 min later it enters the cusp proper, defined by higher fluxes of more isotropic electrons and magnetosheath proton precipitation showing typical energy-latitude and pitch-angle-latitude dispersions [*Smith and Lockwood*, 1996]. The oxygen outflow shows the typical cleft ion fountain energy-latitude dispersion signature and proton outflow also continues (panel d). During the 2-min-long interval prior to the equatorward boundary of the cusp proper, FGM observes a large variation of the B_y component with amplitude about 20 nT, indicating a relatively strong field-aligned current. This field-aligned current is not collocated with the observed local ion heating in the cleft. The ELF electric field variations observed throughout the cusp interval and during the subsequent mantle crossing show an overall gradual decline in the power spectral density with time. Relatively strong low-frequency magnetic field fluctuations are more localized and exist only inside the region with the strongest magnetosheath particle precipitation during the interval 1250:30–1252:30 UT. However, the distribution of the magnetic wave power with frequency is different in the cusp proper than in the cleft, with most of the power at frequencies above 10 Hz (above the H^+ and O^+ gyrofrequencies). Despite the apparent occurrence of electromagnetic and electrostatic waves in the cusp, strong transverse ion energization (90° pitch angle particles) is not detected at this time and oxygen outflow remains in the form of strongly anti-field-aligned beam (discussed in more detail by *Bogdanova et al.* [2004]).

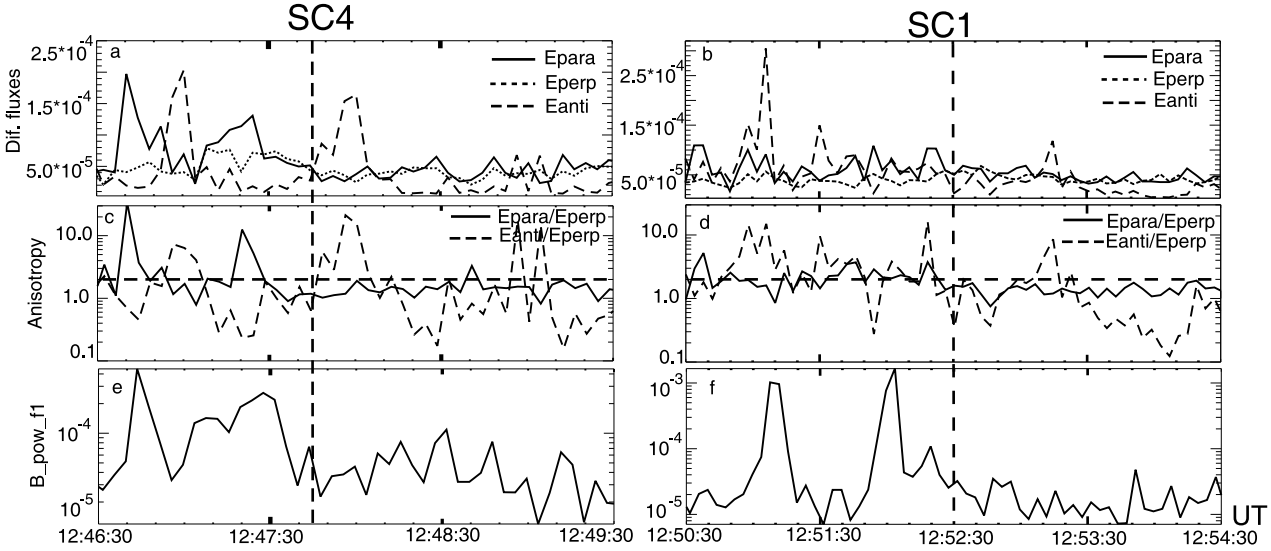

Figure 2. Suprathermal electron beams and extra-low-frequency electromagnetic waves inside the electron-only cleft region, data from spacecraft 4 (left) and spacecraft 1 (right). Figures 2a and 2b present differential energy fluxes, in the parallel (solid line), antiparallel (dashed) and perpendicular (dotted) directions. In this plot we have used the maximum values of the electron fluxes over HEEA energy range. Figures 2c and 2d show an estimation of the anisotropy in the differential energy fluxes: the ratio of field-aligned fluxes to perpendicular fluxes (solid) and anti-field-aligned fluxes to perpendicular fluxes (dashed). Last panels are similar to Figure 1, panel f. The dashed line shows the end of the heating region defined from the ion distributions.

[13] Spacecraft C1 encounters the OCB 4 min after C4, at 1250:30 UT, MLT = 1347, ILAT = 78.0° (indicated by the first dashed line in the right panels). Note that there is only a small difference in location of the C1 and C4 OCB crossings, 0.2° in invariant latitude and 5 min in MLT and 0.15 R_E in altitude. The spacecraft thus follow similar trajectories. C1 observes each of the regions and features described above for the C4 crossing, including local transverse heating of H^+ and O^+, accompanied by enhanced electromagnetic wave power at about 1252:00 UT (and possibly at 1251:10 UT). However, the detected electron and ion differential energy fluxes seen on C1 are significantly less intense, some threefold lower than for C4. Moreover, the maximal energy of the upwelling O^+ ions observed on C1 was 1 keV, in comparison with 2 keV observed on C4. The integrated field-aligned electron number flux is still a few times 10^7 (cm^2 s sr)$^{-1}$. We note that both fluxes of downgoing electrons and fluxes of ions upwelling from the ionosphere toward midaltitudes are weaker on C1 than C4. However, the magnetic field wave power in the 1–10 Hz range detected at C1 during local transverse heating events (90° pitch angle ions) was higher than at C4.

[14] Figure 2 presents data from the PEACE and STAFF instruments for time intervals which start at the OCB, include the heating region and extend further into the cleft. The left panel shows data from C4 (1246:30–1249:30 UT) and the right panel presents data from C1 (1250:30–1254:30 UT). The dashed line marks the poleward boundary of the heating region defined by changes in the ion distributions (no more ions with 90° pitch angles). The top panels show the differential energy flux of the energy band with the most intense flux of the downgoing (solid line) and upgoing electrons (dashed) and of those moving perpendicular to the magnetic field (dotted). The middle panels present an estimation of the electron anisotropy based on the ratio of the differential energy fluxes: field-aligned fluxes to perpendicular fluxes (solid) and anti-field-aligned fluxes to perpendicular fluxes (dashed). For the anisotropy calculation we divided the maximal value of the parallel (antiparallel) differential energy flux to the perpendicular flux value at the same energy. The lower panels are similar to Figure 1, panel f. The background level of the total magnetic field power spectral density was 1×10^{-5} nT^2 Hz^{-1} for C1 and a little more for C4. We have used different scales for C4 and C1. Inside the heating region the C4 data show a strong downgoing (parallel) electron beam at 1246:45 UT and a longer lasting beam centered at 1247:20 UT which occur at the same time as enhancements in the magnetic field power spectral density and enhancement of the local ion heating. The first electron beam has a peak differential energy flux of 2.0×10^{-4} ergs (cm^2 s sr eV)$^{-1}$ and field-aligned anisotropy $E_{II}/E_{perp} \sim 26$. The second electron beam has a peak flux of 1.3×10^{-4} ergs (cm^2 s sr eV)$^{-1}$ and field-aligned anisotropy ~11. A strong upgoing electron beam was observed at 1247:00 UT but without clear correlation with enhancement of the magnetic field power spectral density. After the heating region the field-aligned anisotropy decreases and remains <2 for the rest of the electron-only cleft region. During this time one strong upgoing electron beam with high flux and anisotropy was observed but this beam correlates neither with ion heating nor with changes in magnetic field wave power. The C1 PEACE data differ from C4; the heating region contains more shorter-duration electron beams in both directions. Inside the heating region the anisotropy of the downgoing electron beams is quite low, $E_{II}/E_{perp} \sim 3-6$ and

fluxes rarely exceed 1×10^4 ergs $(cm^2\ s\ sr\ eV)^{-1}$. There are no correlations between downgoing electron beams and two sharp spikes in the magnetic field power spectral density observed at 1250:50–1251:10 UT and 1251:40–1252:30 UT. Similarly to C4, outside the heating region the field-aligned anisotropy was <2. Four upgoing beams were detected, three inside and one outside of the heating region. Only the strongest beam, observed at 1251:10 UT, which has peak anti-field-aligned differential energy flux of 3.5×10^{-4} ergs $(cm^2\ s\ sr\ eV)^{-1}$ and anisotropy around 11, coincides with a strong peak in magnetic field wave power. The other upgoing beams with lower fluxes and/or anisotropy do not correlate with significantly enhanced magnetic field wave power.

3. Discussion and Conclusion

[15] We present a one-event study of the correlation between electron beams, ion heating, and enhancement of the wave activity inside the electron-only cleft region at midaltitudes. The equatorward part of this region consists of strong electron beams in the antiparallel and field-aligned directions. Downgoing beams are magnetosheath electrons from a reconnection site at the magnetopause. Possible reasons for the presence of the upgoing beams include mirroring of the magnetosheath electrons at lower altitudes, or acceleration by downward parallel electric fields below the spacecraft (similar to diverging shocks in the nightside auroral region) if present, or acceleration by small-scale Alfvén waves [*Chaston et al.*, 2003]. The properties of the field-aligned (i.e., downgoing) electron beams observed by Cluster at 4–5 R_E are similar to suprathermal electron bursts (STEB) observed in the nightside auroral region [*Johnstone and Winningham*, 1982] and in the cusp/cleft region at 1400 km altitude [*Knudsen et al.*, 1998].

[16] The beams we observed are colocated with upflowing ionospheric H^+ and O^+ ions conics with pitch angles 90°–180°, suggesting that Cluster passes inside a heating region. Note that in this and other cases we examined, the ion heating region is localized inside the electron-only cleft and the most intense heating disappears before Cluster observes the first magnetosheath ion injections.

[17] The wave data show transient sharp enhancements of the extra-low frequency 1–10 Hz electric and magnetic field wave power just poleward of the OCB, with a strong correlation between the broadband magnetic field wave power and ion conics. This correlation, together with the absence of the low-frequency magnetic field wave power outside the heating region in nearly all cases examined suggests that electromagnetic waves are responsible for the ion heating, e.g., BBELF waves [*André et al.*, 1998], and/or electromagnetic ion-cyclotron waves [*Moore et al.*, 1999a], and/or Alfvén waves [*Knudsen and Wahlund*, 1998]. The identification of the electromagnetic wave modes will be the subject of further study. ELF electric field fluctuations were observed throughout the cleft/cusp/mantle intervals with power spectral density much higher than the background level and with a gradual decrease in power with time. Neither ion injections nor strong field-aligned currents (in comparison with the later cusp field-aligned current) were observed within the heating region, and probably we can conclude that the structured electron precipitations (suprathermal electron bursts) are the most likely the free energy source for wave activity inside the electron-only cleft.

[18] *Knudsen et al.* [1998] estimate the integrated field-aligned electron number flux threshold above which signs of strong ion heating appear at 1400 km as a few times 10^7 $(cm^2\ s\ sr)^{-1}$. Cluster PEACE observations at 3.9–4.5 R_E show a similar level of field-aligned electron number fluxes inside the ion heating region. However, the same fluxes (or even higher) were observed in the cusp proper without ion heating, and thus we think that an electron anisotropy may be essential for the wave generation and ion heating. Our single event study shows that downgoing electron beams with ratios of parallel to perpendicular differential energy fluxes greater than 10 correlate with extra-low frequency 1–10 Hz magnetic field wave power on C4. Transverse ion heating was observed on C4 and C1 only in the regions with electron field-aligned anisotropy greater than 2. Our observations also show no clear correlation between ELF magnetic field wave power/ion heating and upgoing electron beams.

[19] Comparison of data from two spacecraft which cross the OCB with ~4 min time separation shows that ion outflow and local ion heating at Cluster altitudes appear on both satellites just after crossing this boundary and is collocated with anisotropic electron injection in the cleft region. There appears to be a correlation between the actual flux levels of these upgoing ions and injected electrons. This gives us the possibility to suggest that electrons play an important role in the local ion heating. However, we should say that we could not prove a causal relationship and speak only about correlation between anisotropic electron beams, electromagnetic waves, and local ion heating.

[20] On the basis of observations presented in this paper and also previous observations of the ion heating region at lower altitudes, we suggest that the ion outflow from the cleft region near the OCB could appear as a response of the ionosphere-magnetosphere system to the injection of the magnetosheath electrons. We suggest that many properties of this ion outflow, such as location, longitudinal and latitudinal size, relative fluxes, dependence on solar wind, and IMF conditions [e.g., *Miyake et al.*, 2002; *Moore et al.*, 1999b] may be related to the properties of the electron injections from the reconnection site.

[21] **Acknowledgments.** This work was sponsored in the UK by the UCL/MSSL Particle Physics and Astronomy Research Council (PPARC) Rolling Grant. CJO acknowledges support via a PPARC Advanced Fellowship. We would like to thank the CDAWeb team for providing the level 2 ACE MAG and ACE Solar Wind Experiment data.

[22] Lou-Chuang Lee thanks the two reviewers for their assistance in evaluating this paper.

References

André, M., and A. Yau (1997), Theories and observations of ion energization and outflow in the high-latitude magnetosphere, *Space Sci. Rev.*, *80*, 27–47.

André, M., et al. (1990), Ion heating by broadband low-frequency waves in the cusp/cleft, *J. Geophys. Res.*, *95*, 20,809–20,823.

André, M., et al. (1998), Ion energization mechanisms at 1700 km in the auroral region, *J. Geophys. Res.*, *103*, 4199–4222.

Arnoldy, et al. (1996), SCIFER—Structure of the cleft ion fountain at 14000 km altitude, *Geophys. Res. Lett.*, *23*, 1869–1872.

Balogh, A., et al. (2001), The Cluster Magnetic Field Investigation: Overview of in-flight perfomance and initial results, *Ann. Geophys.*, *19*, 1207–1217.

Bogdanova, Y. V., et al. (2004), Investigation of the source region of ionospheric oxygen outflow in the cleft/cusp using multi-spacecraft

observations by CIS onboard Cluster, *Adv. Space Res.*, *34*, 2459–2464.
Bouhram, M., et al. (2002), Ion outflow and associated perpendicular heating in the cusp observed by Interball Auroral Probe and Fast Auroral Snapshot, *J. Geophys. Res.*, *107*(A2), 1023, doi:10.1029/2001JA000091.
Bouhram, M., et al. (2003), Modelling transverse heating and outflow of ionospheric ions from the dayside cusp/cleft. 1. Parametric study, *Ann. Geophys.*, *21*, 1773–1791.
Chaston, C. C., et al. (2003), Properties of small-scale Alfvén waves and accelerated electrons from FAST, *J. Geophys. Res.*, *108*(A4), 8003, doi:10.1029/2002JA009420.
Cornilleau-Wehrlin, N., et al. (2003), First results obtained by the Cluster STAFF experiment, *Ann. Geophys.*, *21*, 437–456.
Dubouloz, N., D. Delcourt, M. Malingre, J.-J. Berthelier, and D. Chugunin (1998), Remote analysis of cleft ion acceleration using thermal plasma measurements from Interball Auroral Probe, *Geophys. Res. Lett.*, *25*, 2925–2928.
Dubouloz, N. D., et al. (2001), Spatial structure of the cusp/cleft ion fountain: A case study using a magnetic conjugacy between Interball AP and a pair of SuperDARN radars, *J. Geophys. Res.*, *106*, 261–274.
Fuselier, S. A., et al. (2002), Localized ion outflow in response to a solar wind pressure pulse, *J. Geophys. Res.*, *107*(A8), 1203, doi:10.1029/2001JA000297.
Gustafsson, G., et al. (1990), On waves below the local proton gyrofrequency in the auroral acceleration region, *J. Geophys. Res.*, *95*, 5889.
Gustafsson, G., et al. (2001), First results of electric field and density observations by Cluster EFW based on initial months of operation, *Ann. Geophys.*, *19*, 1219–1240.
Johnstone, A. D., and J. D. Winningham (1982), Satellite observations of suprathermal electron bursts, *J. Geophys. Res.*, *87*, 2321–2329.
Johnstone, A. D., et al. (1997), Peace: a plasma electron and current experiment, *Space Sci. Rev.*, *79*, 351–398.
Knudsen, D. J., and J.-E. Wahlund (1998), Core ion flux bursts within solitary kinetic Alfven waves, *J. Geophys. Res.*, *103*, 4157–4170.
Knudsen, D. J., J. H. Clemmons, and J.-E. Wahlund (1998), Correlation between core ion energization, suprathermal electron bursts, and broadband ELF plasma waves, *J. Geophys. Res.*, *103*, 4171–4186.
Lockwood, M., et al. (1985), The Cleft Ion Fountain, *J. Geophys. Res.*, *90*, 9736–9748.
McCrea, I. W., M. Lester, T. R. Robinson, and N. M. Wade (1991), On the identification and occurrence of ion frictional heating events in the high-latitude ionosphere, *J. Atmos. Terr. Phys.*, *53*, 587–597.
McCrea, I. W., M. Lockwood, J. Moen, and F. Pitout (2000), ESR and EISCAT observations of the response of the cusp and cleft to IMF orientation changes, *Ann. Geophys.*, *18*, 1009–1026.
Miyake, W., T. Mukai, and N. Kaya (2002), Relationship of upflowing ion beams and conics around the dayside cusp/cleft region to the interplanetary conditions, *Ann. Geophys.*, *20*, 471–476.
Moore, T. E., R. Lundin, D. Alcayde, M. Andre, S. B. Canguli, M. Temerin, and A. Yau (1999a), Source processes in the high-latitude ionosphere, *Space Sci. Rev.*, *88*, 7.
Moore, T. E., et al. (1999b), Ionospheric mass ejection in response to a coronal mass ejection, *Geophys. Res. Lett.*, *26*, 2339–2342.
Newell, P. T., and C.-I. Meng (1998), The cusp and the cleft/boundary layer: Low-altitude identification and statistical local time variation, *J. Geophys. Res.*, *93*, 14,549–14,556.
Nilsson, H., S. Kirkwood, and T. Moretto (1998), Incoherent scatter radar observations of the cusp acceleration region and cusp field-aligned currents, *J. Geophys. Res.*, *103*, 26,721–26,730.
Norqvist, P., M. André, and M. Tyrland (1998), A statistical study of ion energization mechanisms in the auroral region, *J. Geophys. Res.*, *103*, 23,459–23,473.
Oeroset, M., M. Yamauchi, L. Liszka, and S. P. Christon (2000), Energetic ion outflow from the dayside ionosphere and its relationship to the interplanetary magnetic field and Substorm activity, *J. Atmos. Sol. Terr. Phys.*, *62*, 485–493.
Ogawa, Y., et al. (2003), Simultaneous EISCAT Svalbard radar and DMSP observations of ion upflow in the dayside polar ionosphere, *J. Geophys. Res.*, *108*(A3), 1101, doi:10.1029/2002JA009590.
Pollock, C. J., et al. (1990), A survey of upwelling ion event characteristics, *J. Geophys. Res.*, *95*, 18,969–18,980.
Pollock, C. J., et al. (1996), SCIFER—Cleft region thermal electron distribution functions, *Geophys. Res. Lett.*, *23*, 1881–1884.
Rème, H., et al. (2001), First multispacecraft ion measurements in and near the Earth's magnetosphere with the identical Cluster ion spectrometry (CIS) experiment, *Ann. Geophys.*, *19*, 1303–1354.
Smith, M. F., and M. Lockwood (1996), Earth's magnetospheric cusps, *Rev. Geophys.*, *34*, 233–260.
Strangeway, R. J., et al. (2000), Cusp field-aligned currents and ion outflows, *J. Geophys. Res.*, *105*, 21,129–21,142.
Temerin, M., and R. L. Lysak (1984), Electromagntic ion cyclotron mode (ELF) waves generated by auroral electron precipitation, *J. Geophys. Res.*, *89*, 2849.
Valek, P. W., et al. (2002), Outflow from the ionosphere in the vicinity of the cusp, *J. Geophys. Res.*, *107*(A8), 1180, doi:10.1029/2001JA000107.
Yau, A. W., et al. (1983), Particle and wave observations of low-altitude ionospheric ion acceleration events, *J. Geophys. Res.*, *88*, 341–355.

M. André, Swedish Institute of Space Physics, Uppsala Division, Box 537, 751 21 Uppsala, Sweden. (mats.andre@irfu.se)

A. Balogh and P. Cargill, Space and Atmospheric Physics, Imperial College, London SW7 2BZ, UK. (a.balogh@ic.ac.uk; p.cargill@imperial.ac.uk)

Y. V. Bogdanova, A. N. Fazakerley, and C. J. Owen, Mullard Space Science Laboratory, Department of Space and Climate Physics, University College London, Holmbury St. Mary, Dorking, Surrey RH5 6NT, UK. (jb@mssl.ucl.ac.uk; anf@mssl.ucl.ac.uk; cjo@mssl.ucl.ac.uk)

J. M. Bosqued and H. Rème, Centre d'Etude Spatiale des Rayonnements, CNRS/UPS, B.P. 4346, 31029 Toulouse Cedex, France. (bosqued@cesr.fr; henri.reme@cesr.fr)

N. Cornilleau-Wehrlin and B. Grison, Centre d'Etude des Environnements Terrestre et Planetaires, CRPE, 10-12 Avenue de l'Europe, 78 140 Velizy, France. (nicole.cornilleau@cetp.ipsl.fr; benjamin.grison@cetp.ipsl.fr)

L. M. Kistler, Space Science Center, University of New Hampshire, Durham, NH 03824, USA. (lynn.kistler@unh.edu)

B. Klecker, Max-Planck Institute fur Extraterrestrische Physik, Giessenbachstrasse, Postfach 1312, 85741, Garching b. Munchen, Germany. (berndt.klecker@mpe.mpg.de)